JID Open

β2-Adrenoceptor Activation Modulates Skin Wound Healing Processes to Reduce Scarring

Gabrielle S. Le Provost[1] and Christine E. Pullar[1]

During wound healing, excessive inflammation, angiogenesis, and differentiated human dermal fibroblast (HDF) function contribute to scarring, whereas hyperpigmentation negatively affects scar quality. Over 100 million patients heal with a scar every year. To investigate the role of the beta 2 adrenergic receptor (β2AR) in wound scarring, the ability of beta 2 adrenergic receptor agonist (β2ARag) to alter HDF differentiation and function, wound inflammation, angiogenesis, and wound scarring was explored in HDFs, zebrafish, chick chorioallantoic membrane assay (CAM), and a porcine skin wound model, respectively. Here we identify a β2AR-mediated mechanism for scar reduction. β2ARag significantly reduced HDF differentiation, via multiple cAMP and/or fibroblast growth factor 2 or basic FGF (FGF2)-dependent mechanisms, in the presence of transforming growth factor betaβ1, reduced contractile function, and inhibited mRNA expression of a number of profibrotic markers. β2ARag also reduced inflammation and angiogenesis in zebrafish and CAMs *in vivo*, respectively. In Red Duroc pig full-thickness wounds, β2ARag reduced both scar area and hyperpigmentation by almost 50% and significantly improved scar quality. Indeed, mechanisms delineated *in vitro* and in other *in vivo* models were evident in the β2ARag-treated porcine scars *in vivo*. Both macrophage infiltration and angiogenesis were initially decreased, whereas DF function was impaired in the β2ARag-treated porcine wound bed. These data collectively reveal the potential of β2ARag to improve skin scarring.

Journal of Investigative Dermatology (2015) **135,** 279–288. doi:10.1038/jid.2014.312; published online 21 August 2014

INTRODUCTION

Wound repair is complex, requiring the coordinated action of numerous cell types and physiological processes to facilitate healing. In contrast to the perfect regeneration in embryonic wounds (Redd *et al.*, 2004), adult wounds heal with fibrotic scars (Shaw and Martin, 2009). Evolution has primed repair processes to heal quickly, but imperfectly (Stramer *et al.*, 2007). Excessive inflammation (Stramer *et al.*, 2007), angiogenesis (DiPietro, 2013), and DF function (Hinz, 2007) all contribute to scarring. Annually, 100 million patients, in the developed world, heal with scars after elective procedures, trauma, and burn injuries, causing serious cosmetic/functional problems, which are emotionally and physically debilitating, placing hefty financial burdens on Healthcare Systems (Bayat *et al.*, 2003).

Beta-adrenergic receptor familys (βARs: β1AR; β2AR; β3AR (Wallukat, 2002)) are G protein–coupled receptors for catecholamines released from the adrenal medulla and sympathetic nervous system (Nagatsu and Stjarne, 1998), but they are also synthesized and secreted by keratinocytes (Pullar *et al.*, 2006b). As βARs are highly expressed on most skin cells, an autocrine (epidermis) and paracrine (dermis) βAR skin network exists (Pullar *et al.*, 2008). Moreover, beta 2 adrenergic receptor agonist (β2ARag) may protect patients from developing venous leg ulcers (Margolis *et al.*, 2007).

βARs can influence wound healing processes. βARag reduced re-epithelialization of clipped mouse tails, where healing lacks a dermal component (Pullar *et al.*, 2006a). In contrast, βAR antagonism promoted skin re-epithelialization (Pullar *et al.*, 2006b) in *ex vivo* models of chronic wound re-epithelialization (Kratz, 1998) and murine skin burn models *in vivo* (Sivamani *et al.*, 2009) and accelerated skin barrier recovery (Denda *et al.*, 2003). Indeed, βAR antagonism and beta 2 adrenergic receptor (*β2AR)* gene deletion both promoted very early stages of murine wound healing *in vivo* (Pullar *et al.*, 2012), and βAR antagonism has successfully healed chronic wounds (Tang *et al.*, 2012; Braun *et al.*, 2013; Lev-Tov *et al.*, 2013; Manahan *et al.*, 2014).

No previous study has addressed the role of β2AR in wound scarring. The β2ARag Salbutamol is a safe and widely used

[1]*Department of Cell Physiology and Pharmacology, University of Leicester, Leicester, UK*

Correspondence: Christine E. Pullar, Department of Cell Physiology and Pharmacology, University of Leicester, PO Box 138, University Road, Leicester LE1 9HN, UK.
E-mail: cp161@le.ac.uk

Abbreviations: α-NAE, α-naphtyl acetate esterase; βAR, beta-adrenergic receptor family; β2AR, beta 2 adrenergic receptor; β2ARag, beta 2 adrenergic receptor agonist; CCN2, connective tissue growth factor; FGF2, fibroblast growth factor 2 or basic FGF; FN EDA, fibronectin (FN) EDA; H&E, hematoxylin and eosin; HDF, human dermal fibroblasts; MFA, mature focal adhesion; PD, PD173074 FGFR inhibitor; PDGF, platelet-derived growth factor; RT-PCR, real-time polymerase chain reaction; SFM, serum-free medium; SMA, smooth muscle α actin; SMFA, supermature focal adhesion; TGFβ, transforming growth factor beta; vWF, von Willebrand factor

Received 25 February 2014; revised 25 June 2014; accepted 9 July 2014; accepted article preview online 22 July 2014; published online 21 August 2014

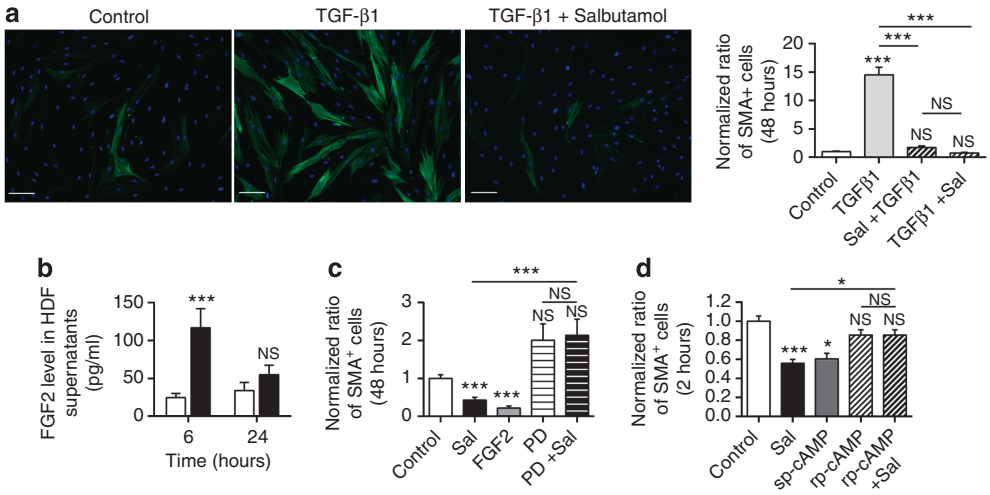

Figure 1. β2AR agonist (β2ARag) reduces human dermal fibroblast (HDF) differentiation and contractile function *in vitro* via cAMP- and fibroblast growth factor 2 or basic FGF (FGF2)-dependent mechanisms. HDFs were treated with serum-free medium (SFM) alone or SFM containing Salbutamol/Formoterol (10 μM), TGFβ1 (1 ng ml^{-1}), FGF2 (10 ng ml^{-1}), PD173074 FGFR inhibitor (PD173074,50 nM), sp-cAMP/rp-cAMP (50 μM), alone or pretreated, as indicated. (**a**) HDFs were treated for 48 hours with TGFβ1 alone or 6 hours pretreatment with TGFβ1 or β2ARag before β2ARag or TGFβ1 addition, respectively, for 42 hours. Ratios of smooth muscle α actin (SMA)-positive cells to total cells were normalized to control. Scale bar = 100 μm. (**b**) HDF FGF2 secretion was ELISA analyzed 6/24 hours post treatment in the presence or absence of β2ARag. (**c**) HDFs were treated for 48 hours with FGF2, PD, or β2ARag, with/without 6 hours of PD pretreatment. (**d**) HDFs were treated for 2 hours with sp-cAMP, rp-cAMP, or β2ARag, with/without rp-cAMP pretreatment, 30 minutes before β2ARag for 2 hours. Data presented are means ± SEM; 4 independent experiments. NS, not significant.

asthma medication (Boskabady and Saadatinejad, 2003). Here, the effect of β2ARag on DF differentiation and function, inflammation (zebrafish wounds) (Renshaw *et al.*, 2006), and angiogenesis (chick chorioallantoic membrane assay (CAM)) (Ausprunk *et al.*, 1974) was investigated. Furthermore, as porcine skin is anatomically similar to human skin (Montagna and Yun, 1964), the effect of Salbutamol on wound scarring was explored in the Red Duroc pig, a widely used model for evaluating human scar reduction interventions (Gallant-Behm *et al.*, 2008).

RESULTS

β2ARag reduces human dermal fibroblast (HDF) differentiation and contractile function *in vitro* via cAMP and fibroblast growth factor 2 or basic FGF (FGF2)-dependent mechanisms

HDF smooth muscle α-actin (SMA) expression, a differentiated fibroblast–myofibroblast marker (Hinz *et al.*, 2001), was analyzed by immunocytochemistry. After 48 hours in basal medium, 1.5% of cells were positive for SMA, whereas partial (Salbutamol, 57%) and full (Formoterol, 39%) β2ARags (Baker, 2010) decreased the ratio of SMA-positive HDFs (Supplementary Figure S1a online). Previously, a nonselective βARag reduced HDF contractile function in floating collagen gels (Pullar and Isseroff, 2005). Here, using restrained-collagen gels, where gel tension promotes differentiation (Tomasek *et al.*, 2002), β2ARag significantly reduced gel contraction (Supplementary Figure S1b online).

Transforming growth factor beta (TGFβ)1, a fibroblast differentiation promoter strongly upregulated in wounds (Hinz, 2007), increased the ratio of SMA-positive HDFs by 14.5-fold (Figure 1a). Regardless of whether the β2ARag was added 6 hours prior or subsequent to TGFβ1 for a further 42 hours, similar, marked inhibition was observed, decreasing the ratio of SMA-positive HDFs by up to 95% (Figure 1a).

A β2ARag-mediated decrease in TGFβ1 secretion could underpin its reduction in HDF SMA expression. TGFβ1 was detected in the HDF supernatant, but there was no β2ARag-mediated effect (Supplementary Figure S2a online). FGF2 can reduce myofibroblast function (Ishiguro *et al.*, 2009; Tiede *et al.*, 2009). β2ARag increased FGF2 secretion by 4.3- and 0.59-fold after 6 and 24 hours, respectively (Figure 1b). Indeed, exogenous FGF2 alone decreased the ratio of SMA-positive HDFs by 79% (Figure 1c). HDFs express the FGF2 receptor fibroblast growth factor receptor1 (Takenaka *et al.*, 2002). Treatment with the fibroblast growth factor receptor1 inhibitor PD173074 (PD) (Miyake *et al.*, 2010) increased the ratio of SMA-expressing HDFs by 2-fold (Figure 1c). Meanwhile, in the presence of PD, β2ARag no longer reduced SMA-positive HDF numbers, both in the presence and absence of TGFβ1 (Figure 1c, Supplementary Figure S2b online).

β2ARs can couple to $G\alpha_s$, increasing intracellular cAMP (Scott *et al.*, 1999). A cAMP analog (sp-cAMP) alone decreased SMA-positive HDFs by 40% (Figure 1d, Supplementary Figure S2c online), whereas a cAMP analog that inhibits protein kinase A (rp-cAMP) (Dostmann *et al.*, 1990) had no significant effect alone, but completely prevented the β2ARag-mediated reduction in SMA-expressing HDFs (Figure 1d, Supplementary Figure S2c online), suggesting that the mechanism was cAMP and protein kinase A dependent.

To investigate downstream signaling through mitogen-activated protein kinases (MAPK), experiments were performed in

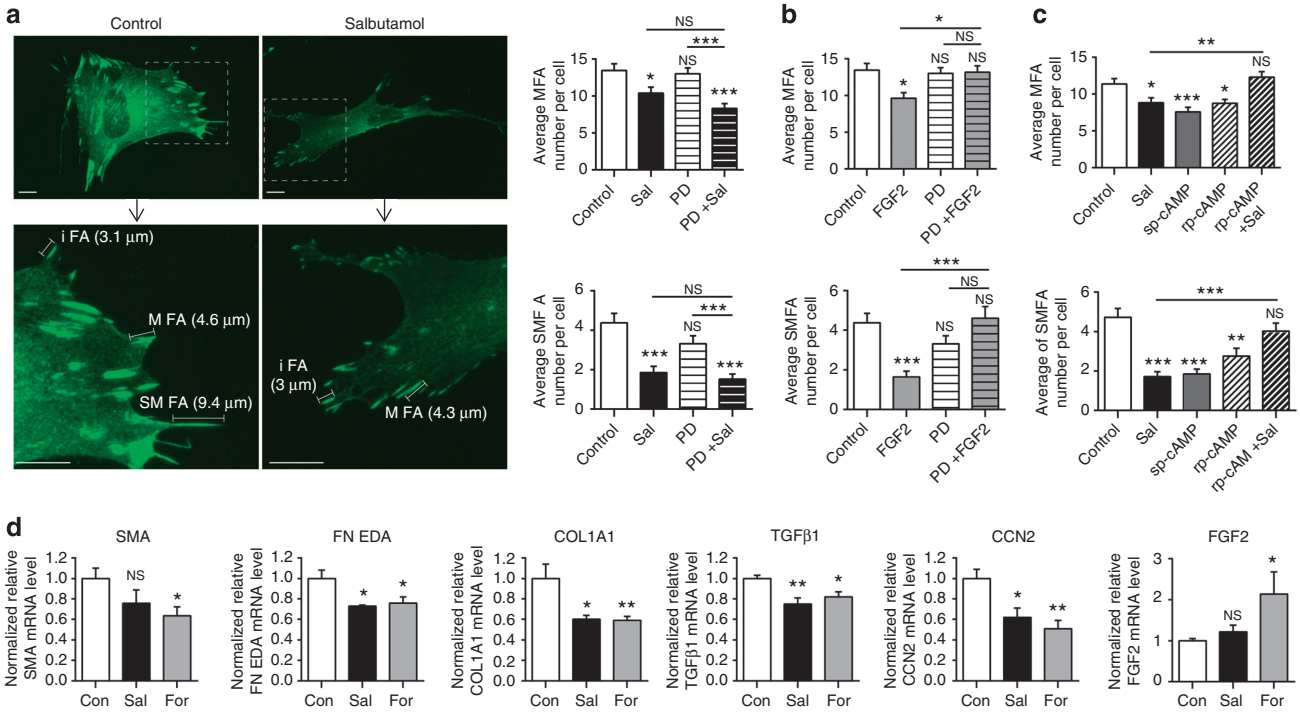

Figure 2. β2AR agonist (β2ARag) reduces the number of mature FAs on the human dermal fibroblast (HDF) periphery and profibrotic gene expression. HDFs were treated with serum-free medium (SFM) alone or containing β2ARag (Salbutamol, 10 μM), fibroblast growth factor 2 or basic FGF (FGF2) (10 ngml^{-1}), PD173074 FGFR inhibitor (PD) (50 nM), sp-cAMP, rp-cAMP (50 μM), alone for 15 minutes or with pretreatment, as indicated. HDFs were pretreated with PD (**a**, **b**) or rp-cAMP (**c**) for 30 minutes, and then with β2ARag (**a**, **c**) or FGF2 (**b**) for a further 15 minutes. Mature (top) and supermature (bottom) FAs were measured and counted. Representative pictures are shown. Scale bar = 10 μm. Data are presented as mean ± SEM from at least 4 independent experiments (*$P<0.05$, **$P<0.01$). HDF gene expression was analyzed by RT-PCR, 6 hours post treatment with β2ARag (Salbutamol, Formoterol, 10 μM), in SFM. Mean mRNA levels were normalized to control values. Data are presented as mean ± SEM from at least four independent experiments (*$P<0.05$, **$P<0.01$). CCN2, connective tissue growth factor; COL1A1, type 1 collagen, alpha 1; FGF2, fibroblast growth factor 2; FN EDA, fibronectin (FN) EDA; NS, not significant; SMA, smooth muscle α actin; TGFβ1, transforming growth factor beta 1.

the presence of selective inhibitors of MEK1/2 (U0126), p38 MAP kinase (SB202190), or JNK (JNK inhibitor VIII, which inhibits JNK1/2/3). Inhibiting the MAP kinases individually had no effect and did not prevent the β2ARag-mediated reduction in the number of SMA-expressing HDFs (Supplementary Figure S2d online).

β2ARag reduces the number of mature focal adhesions on the HDF periphery and profibrotic gene expression

Tension is a major driver of fibroblast differentiation (Hinz, 2007). Mature focal adhesions (MFAs) facilitate tension-sensing in the immediate fibroblast environment. Within high-tension, healing wounds, differentiating fibroblasts develop larger SMFAs (8–30 μm), with superior contractile ability compared with MFAs (4–8 μm) (Dugina *et al.*, 2001).

To determine whether β2ARag altered the number of M/supermature focal adhesion (SMFAs), the length of FAs at the HDF periphery was analyzed. β2ARag reduced both peripheral HDF MFA and SMFA numbers by 23 and 58%, respectively (Figure 2a). PD was used to probe FGF2 involvement, and it had no effect alone and it did not prevent the β2ARag-mediated reduction in M/SMFA numbers (Figure 2a). However, exogenous FGF2 also reduced HDF peripheral MFA and SMFA numbers by 29 and 63%, respectively, whereas PD completely prevented any decrease (Figure 2b).

Similar to the SMA studies above, the use of rp-cAMP prevented the β2ARag-mediated reduction in M/SMFA numbers, demonstrating that the underpinning mechanism was cAMP dependent (Figure 2c) but independent of MAP kinases (Supplementary Figure S2e online). Overall, β2ARag reduced M/SMFA numbers directly via cAMP-mediated and indirectly via FGF2-mediated (Figure 1b) pathways. Additional experiments demonstrated that the β2ARag-mediated reduction in gel contraction was also partly FGF2 dependent (Supplementary Figure S2f online).

To determine whether β2ARag altered HDF profibrotic capability, RT-PCR was performed for profibrotic genes (Hinz, 2007). Salbutamol and Formoterol decreased SMA, fibronectin (FN) EDA, type I collagenA1, TGFβ1, and connective tissue growth factor (CCN2) gene expression by 24 to 49% and increased FGF2 gene expression by 1.2- and 2.1-fold, respectively, after 6 hours (Figure 2d). No effects on TGFβ2, TGFβ3, COL1A2, PDGF-A, MMP2, or decorin gene expression were observed (results not shown). In addition, whereas TGFβ1 decreased HDF β2AR gene expression by 73%, FGF2 increased β2AR expression by 1.5-fold

(Supplementary Figure S2g online). Apart from the β2ARag-mediated increase in FGF2 gene expression, all changes were independent of FGF2 (Supplementary Figure S2h online).

β2ARag reduces zebrafish inflammation and embryonic chick angiogenesis

Excessive wound inflammation contributes to scarring (Stramer *et al.*, 2007). A zebrafish tail wound model was used to visualize neutrophil guidance to wounds in real time (Renshaw *et al.*, 2006). β2ARag reduced neutrophil recruitment by 60% after 6 hours (Supplementary Figure S3a online).

Although angiogenesis is essential for wound repair, reduced angiogenesis is linked with improved healing (DiPietro, 2013) and less angiogenesis occurs in nonscarring oral wounds (Szpaderska *et al.*, 2005) and scarless fetal wounds (Wilgus *et al.*, 2008). β2ARag significantly reduced angiogenesis in the chick chorioallantoic membrane assay (CAM) by 29% (Supplementary Figure S3b online).

β2ARag altered the open wound area within the first 14 days of wound healing but did not affect the re-epithelialization of full-thickness Red Duroc pig wounds

The effect of β2ARag on wound scarring was tested in a porcine skin wound model. Similar to humans, Red Durocs heal wounds with excessive collagen fiber formation (Gallant-Behm and Hart, 2006), generating raised hyperpigmented scars (Gallant *et al.*, 2004). Twenty full-thickness wounds were created along each back (Figure 4a); pigs were randomized and treated daily with vehicle alone or containing 5 mM Salbutamol sulfate. Two wounds/animal were biopsied weekly initially (7/14/21/28/42 days post wounding), and all wounds were digitally photographed. Remaining scars were photographed and collected 56 days post wounding.

Calibrated digital wound pictures were used to determine the open wound area. β2ARag-treated open wound area was 11% smaller and appeared less red and swollen than controls, at 7 days post wounding (Figure 3a). After 14 days, β2ARag-treated open wound area was 23% larger, but there was no significant difference in the open wound area after 28 days, when wounds were almost completely healed (Figure 3a). Re-epithelialization rates could not be assessed 7 days post wounding, but they were similar in both groups after 14 or 28 days and almost all wounds were completely re-epithelialized by 28 days post wounding (Figure 3b).

β2ARag reduces scar area and improves the appearance of Red Duroc scars

Scars were visible from day 28 onward, and scar area was measured from calibrated digital pictures in a double-blind manner. One scar (1–10, control/β2ARag, Figure 4a), closest to the average scar area at that position, is presented alongside a mask delineating scar area (Figure 4b). β2ARag reduced scar area by 34, 38, and 47%, 28, 42, and 56 days post wounding, respectively (Figure 4c). Tension worsens scarring (Ogawa *et al.*, 2011) and varies along the porcine back, with the highest tension most caudally (positions 9/10). Indeed, wounds in positions 9/10 had scars almost twice the size of wounds in the most cranial positions, 1/2 (Figure 4b and d). Moreover, β2ARag reduced scar area by 50% in the highest tension positions (9/10) (Figure 4d).

Scar appearance, evaluated by hyperpigmentation, color match, sheen, height, texture, and pliability, was scored in a double-blind manner (Supplementary Table S1 online). The three less pigmented wounds at position 10 in both groups are presented (Figure 4e). β2ARag improved pigmentation (48%), color match (44%), sheen (53%), height (34%), texture (22%), and pliability (22%) (Figure 4f). Furthermore, hyperpigmentation was maximal in wounds at positions of highest tension (9/10) and significantly improved at all scar positions in the β2ARag-treated pigs (Figure 4g).

Immunohistochemistry reveals a reduction in profibrotic mechanisms underpinning the β2ARag-mediated scar reduction

Wound inflammation was investigated using both the macrophage α-naphtyl acetate esterase (α-NAE) stain and an anti-macrophage antibody, CD163, specific for the M2 alternatively activated/healer macrophages (Weisser *et al.*, 2013). α-NAE staining revealed an 18% decrease in biopsy macrophage-infiltrated area, after 7 days, in β2ARag-treated wounds (Figure 5a). In contrast, after 14 days, β2ARag treatment increased the macrophage-infiltrated area by 28% (Figure 5a). From 21 to 56 days post wounding, there was no difference in macrophage-infiltrated area between groups (Figure 5a). At 14 days post wounding, CD163-specific staining appeared similar to the α-NAE staining (Figure 5b).

Discrete blood vessels were detected by anti-von Willebrand factor (vWF) immunohistochemistry and counted within defined areas of biopsies/excised scars. After 7 days, the number of discrete vWF-stained structures decreased by 22% in β2ARag-treated biopsies (Figure 5c). Similar to the pattern observed with macrophage infiltration, β2ARag increased discrete vWF-stained structure density by 2-fold, after 14 days (Figure 5c). In contrast, after 21/28/42 days, discrete vWF-stained structure densities were lower in β2ARag-treated biopsies (Figure 5c). By 56 days post wounding, angiogenesis was markedly reduced in all wounds, and there was no difference in vWF-stained structure density between groups at the end of study (Figure 5d). Biopsies were stained with the proliferation marker Ki67, but no differences were observed between groups (results not shown).

Collagen deposition and fiber formation were analyzed by histology on cranial–caudal cross-sections of whole excised scars to observe the entire wound bed, 56 days post wounding. Masson's trichrome stain was used to detect the presence (green) and absence (red) of collagen fibrillar structures within the wound bed. In β2ARag-treated wounds, the area without collagen fibers was 1.5-fold larger than in control-treated wounds (Figure 5e), but there was no difference in COL1 staining between groups (Supplementary Figure S4a online).

Biopsies, from day 14 onward, were positively stained for SMA and FN EDA, markers of DF profibrotic phenotype (Hinz, 2007). The wound bed area positively stained for SMA and FN EDA was almost halved in β2ARag-treated scars (Figure 5f and g). However, there was no difference in COL3 (not shown) or CCN2 (downstream of TGFβ1) staining between groups (Supplementary Figure S4b online). To investigate

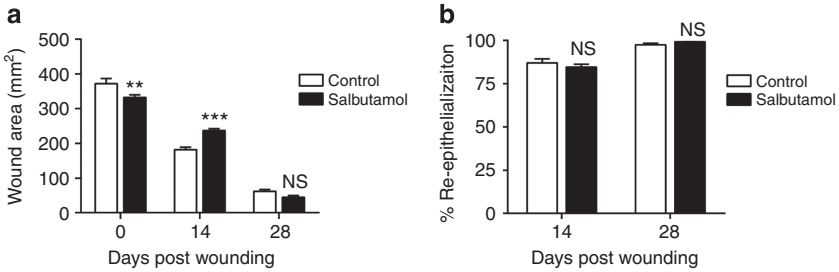

Figure 3. β2AR agonist (β2ARag) altered the open wound area within the first 14 days of wound healing but did not affect the re-epithelialization of full-thickness Red Duroc pig wounds. (**a**) Calibrated photographs of wounds per position were analyzed and wound area was measured at days 0, 7, 14, and 28 in a double-blind manner, as described in the Methods. (**b**) Percentage of re-epithelialization was determined at days 14 and 28 in a double-blind manner, as described in Materials and Methods. Values presented are means ± SEM (10 wounds/animal; $N=5$, $^{*}P<0.05$; $^{**}P<0.01$; $^{***}P<0.001$). NS, not significant.

underpinning mechanisms for reducing fibroblast differentiation, FGF2 staining was performed on excised scars. FGF2 staining intensity was 2-fold higher in the β2ARag-treated wound bed (Figure 5h).

DISCUSSION

β2ARag restrained mechanisms that contribute to scarring, including HDF differentiation and function *in vitro*, and inflammation (zebrafish) and angiogenesis (chick chorioallantoic membrane assay (CAM)) *in vivo*. Moreover, in Red Duroc pigs, Salbutamol significantly reduced wound scarring by 47%, 56 days post wounding. Histology confirmed that β2ARag initially reduced inflammation and angiogenesis, whereas DF function was restrained in the wound dermis. Indeed, at the end of study, scar area and hyperpigmentation were reduced by almost half, and scar appearance was significantly improved in β2ARag-treated wounds compared with controls.

In vitro, β2ARag reduced HDF profibrotic nature by impairing their ability to sense tension within the wound (reduced peripheral MFA and SMFA numbers) and reduced profibrotic gene expression (SMA, FN EDA, TGFβ1, CCN2, type I collagenA1), leading to a reduction in differentiation via cAMP and/or FGF2 dependent and MAPK-independent mechanisms, resulting in reduced contractile function (Figures 1 and 2, Supplementary Figures S1 and S2 online). Indeed, β2ARag increased HDF FGF2 mRNA expression and secretion *in vitro* (Figures 1b and 2d) and increased FGF2 staining intensity in excised scars (Figure 5h).

Recently, cAMP was highlighted as a regulator in tissue fibrosis (Insel *et al.*, 2012) and FGF2, highly expressed in scarless fetal skin (Chen *et al.*, 2006), reduced scarring in human acute incisional wounds (Ono *et al.*, 2007). The β2AR-mediated increases in cAMP and FGF2 were likely highly beneficial in steering wound healing toward regeneration and away from scarring in the porcine full-thickness wounds.

Here, β2ARag reduced inflammatory cell guidance to zebrafish wounds *in vivo* within hours post wounding (Supplementary Figure S3a online) and reduced the macrophage-infiltrated area in 7-day porcine wound biopsies, the earliest time point that biopsies could be taken from the porcine wound edge (Figure 5a). However, the macrophage-infiltrated area was actually 28% larger in β2ARag-treated wounds, 14 days post wounding, compared with controls, whereas there was no difference from day 21 onward (Figure 5a). The main macrophage phenotypes, characterized in murine models, are classically activated killer macrophages (M1), or alternatively activated healer macrophages (M2) (Weisser *et al.*, 2013), although subsets of these phenotypes exist in wounds (Sindrilaru and Scharffetter-Kochanek, 2013). Murine M2 can be identified by CD163 expression, also identified on pig macrophage populations (Fairbairn *et al.*, 2013). In the present study, the pattern of macrophage staining with α-NAE and CD163 was identical 14 days post wounding, suggesting that all biopsy macrophages expressed CD163 (Figure 5b). Therefore, either M2 alone is recruited to porcine wounds, perhaps contributing to the β2ARag-mediated scar reduction, or CD163 is not a phenotype-specific pig M2 marker. The effect of β2ARag on angiogenesis and macrophage infiltration appeared highly correlated (Figure 5a and b). M2 macrophages promote wound angiogenesis (Lucas *et al.*, 2010), and macrophages are necessary to stimulate and fuse tip cells at the leading edge of angiogenic sprouts (Fantin *et al.*, 2010). It is possible that the β2ARag-mediated increase in CD163-expressing macrophages, 14 days post wounding, facilitated the large increase in angiogenesis observed in the β2ARag-treated wounds at this time point.

β2ARag-treated and control wounds re-epithelialized at the same rate from day 14 onward (Figure 4b). Previously, an early βARag-mediated delay in murine skin wound re-epithelialization was observed (Pullar *et al.*, 2006a; Sivamani *et al.*, 2009). Perhaps we missed an early delay in this study. Rodent skin is untethered, however, and wounds heal primarily by wound contraction (Hayward and Robson, 1991); therefore, a βAR-mediated reduction in wound contraction (Pullar and Isseroff, 2005) (Figure 3a) could have underpinned this delay in murine models. In contrast, porcine and human skin wounds close primarily by wound re-epithelialization (Sullivan *et al.*, 2001).

Histology confirmed that β2ARag had restrained DF differentiation in excised scars; the area of the dermis stained for SMA/FN EDA was significantly reduced, whereas FGF2 staining intensity was increased 2-fold (Figure 5f–h). In addition, after 14 days, β2ARag-treated wounds were larger, suggesting a reduction in wound contraction. Mechanisms delineated *in vitro*, underpinning the β2ARag-mediated reduction in DF differentiation/function, appeared operational *in vivo*

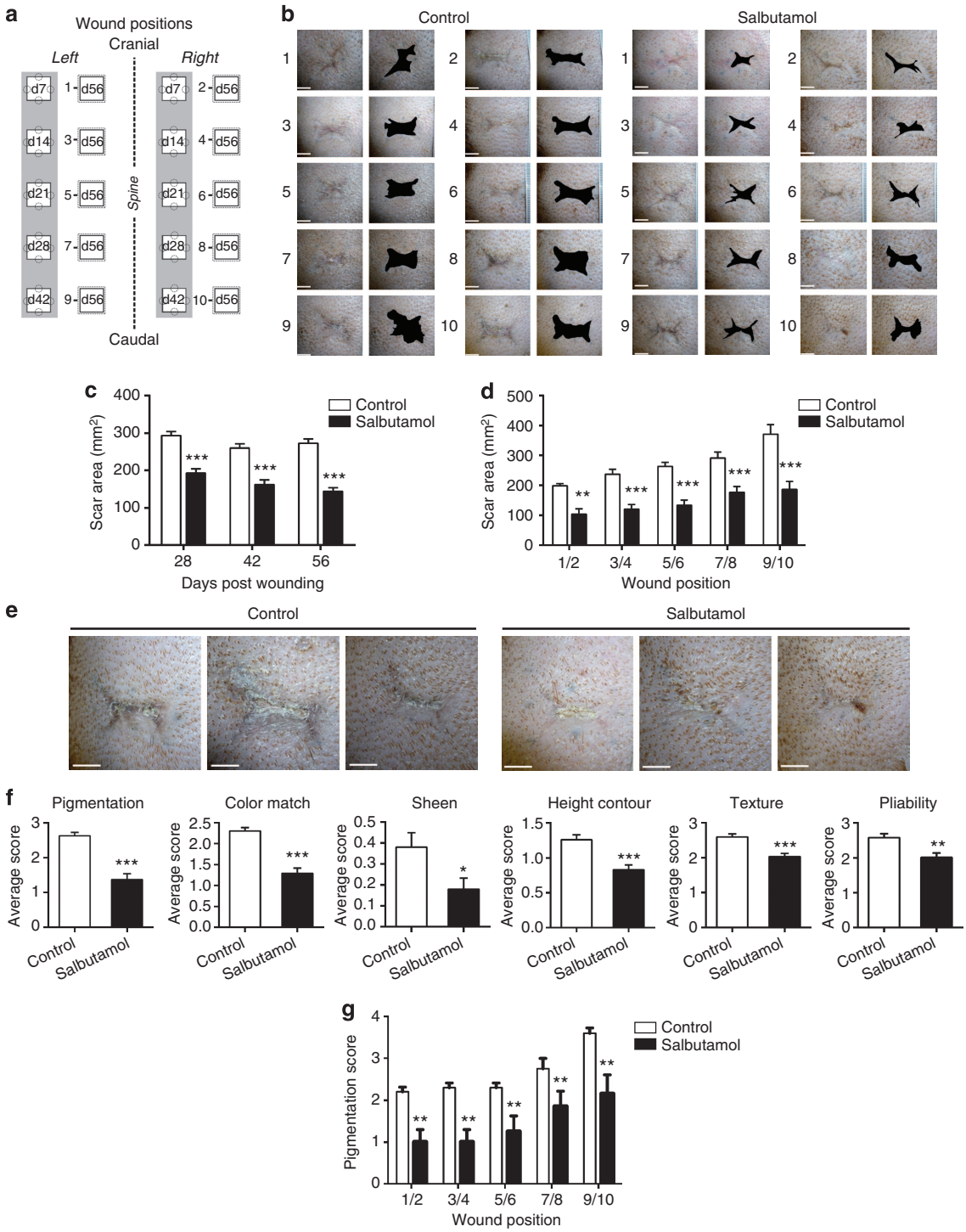

Figure 4. β2AR agonist (β2ARag) reduces scar area and improves the appearance of Red Duroc scars. (**a**) Twenty $2 \times 2\ cm^2$ full-thickness wounds were photographed (7, 14, 21, 28, and 42 days post wounding (gray columns)); four 6-mm punch biopsies (dotted circles) were collected from each edge of two wounds for histology. At day 56, the remaining scars (positions 1–10) were photographed and, after euthanasia, excised for histology (dotted squares). (**b**) Representative pictures shown, closest to mean scar area at positions 1–10, in the absence (left)/presence (right) of a mask delineating scar area and used for measurement ($N = 5$). Scale bar = 1 cm. (**c**, **d**) Scar areas were measured 28, 42, and 56 days post wounding from calibrated pictures, in a double-blind manner. (**d**) Scar area/position is presented 56 days post wounding. (**e**,**f**,**g**) 56 Days post wounding; representative calibrated pictures of the three least hyperpigmented scars/group, position 10 are presented. Scale bar = 1 cm (**e**). Scar characteristics were double-blind scored, using a porcine scar scale, Supplementary Table S1 online (**f**). Hyperpigmentation scores are presented per position (**g**). Data presented are means ± SEM (10 scars/animal; $N = 5$, $^*P < 0.05$; $^{**}P < 0.01$; $^{***}P < 0.001$).

(Figure 5f–h). Moreover, Masson's trichrome staining revealed a 1.5-fold increase in wound bed area without collagen fibers, but no significant difference in the collagen I staining, suggesting that β2ARag had not altered collagen I deposition in the neodermis but had delayed the incorporation of collagen I into fibers (Figure 5e, Supplementary Figure S4a online). Keloids and hypertrophic scars contain a large increase in collagen fibers and bundles (Tuan and Nichter, 1998); therefore, the β2ARag-mediated reduction in collagen fiber formation perhaps contributed to the reduced scar area and improved scar appearance.

β2ARag also reduced scar hyperpigmentation and improved sheen, height, texture, and pliability (Figure 4). Indeed, knockdown of Adrb2a, a β2AR ortholog expressed in zebrafish brain and epidermis, induced significant hypopigmentation, revealing a functional β2AR role in pigmentation (Wang *et al.*, 2009). Inflammation is essential for zebrafish wound hyperpigmentation (Levesque *et al.*, 2013). Here, β2ARag reduced inflammation (Supplementary Figures S3a, Figure 5a and b online), which could have contributed to the reduced hyperpigmentation; future work will address this.

In conclusion, our work highlights the β2AR as a regulator of wound healing/scarring. There are currently no clinically tested or licensed interventions/pharmaceuticals available to reduce wound scarring/fibrosis or to improve scar hyperpigmentation. Topical Salbutamol significantly improved acute skin scarring *in vivo* and could have significant potential as a treatment. Future work will address the potential to improve hypertrophic scarring, keloid formation, and organ fibrosis.

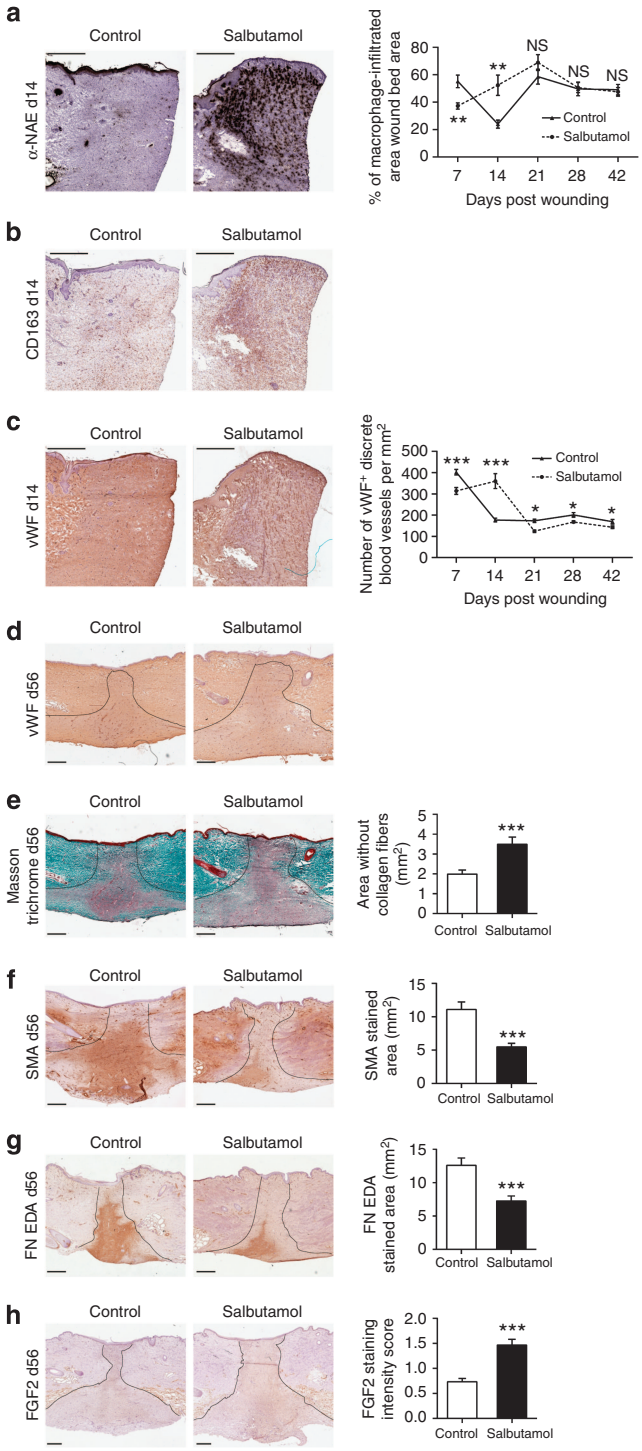

MATERIALS AND METHODS

Ethics statement

Scar study was performed under UK Home Office License (40/3535). Local ethics approval was obtained from The University of Nottingham ACUC.

Animals

Adult zebrafish were maintained in compliance with the Animals (Scientific Procedures) Act, 1986. Embryos were collected and raised in 28.5 °C egg water until the required developmental stage (Westerfield, 1994; Kimmel *et al.*, 1995).

Ten female, 3-month-old Red Duroc pigs (30–35 kg) were purchased from a certified breeder. Animals were acclimatized the week before study commencement and were maintained on a standard diet.

Cell culture

Three HDF strains (Invitrogen, Paisley, UK), passages 3–15, were used throughout. HDFs were maintained at 37 °C in a humidified atmosphere of 5% CO_2, as subconfluent monolayers in fibroblast complete

Figure 5. Immunohistochemistry (IHC) reveals a reduction in profibrotic mechanisms underpinning the β2AR agonist (β2ARag)-mediated scar reduction. α-Naphtyl acetate esterase (α-NAE) staining (all biopsies) (**a**) and CD163 IHC (day 14 biopsies) (**b**) determined the percentage of wound bed macrophage-infiltrated area. Angiogenesis was assessed by von Willebrand factor (vWF) IHC (all biopsies) (**c**) and day 56 excised scars (**d**). vWF-positive discrete blood vessel density was determined within defined wound bed areas. Masson's trichrome staining, smooth muscle α actin (SMA), fibronectin (FN) EDA, and fibroblast growth factor 2 or basic FGF (FGF2) IHC were performed on day 56 excised scars. Wound bed area (defined from H&E staining (not shown)) without collagen fibers (red) was measured. (**e**) SMA and FN EDA positive-stained wound bed area was measured (**f**, **g**). FGF2 expression was evaluated using an intensity score (0–2) (**h**). Representative figures and graphical quantification are shown (2 biopsies/$N = 5$ (biopsies); 10 scars/$N = 5$ (excised scars)). Lines demarcate the wound bed. Scale bar = 1 mm. Data are presented as mean ± SEM (*$P < 0.05$, **$P < 0.01$, ***$P < 0.001$). NS, not significant.

medium: Dulbecco's modified Eagle's medium, 0.5% antibiotic solution, and 10% fetal bovine serum (Invitrogen). Sometimes serum-free medium (SFM) was used. All drugs were purchased from Tocris (Bristol, UK), except FGF2 and TGFβ1 (Promocell, Heidelberg, Germany).

Quantitative RT-PCR

11,500 HDFcm^{-2} were plated into dishes, reaching 80% confluency within 48 hours, and then serum-starved overnight, before treatment in SFM alone or supplemented with Salbutamol or Formoterol (10 μM). At 6 hours post treatment, total RNA was isolated (Nucleospin RNA II kit, Macherey Nagel, Duren, Germany) with DNase treatment. A measure of 1 μg of total RNA was reverse-transcribed using oligo-dT (NanoScript RT kit, Primer Design, Southampton, UK). Duplicate PCR reactions were performed with 10 ng of cDNA, 300 nM primers, and SYBR green Precision MasterMix (Primer Design) on a LightCycler 480 (Roche, Welwyn, UK), followed by a melting curve. Type I collagenA1, CCN2, FGF2, SMA, and TGF-β1 primers were purchased from Primer Design, whereas primers for β2AR and FN EDA were custom-designed using NCBI Primer Blast and synthesized by Sigma-Aldrich (Gillingham, UK). Reference genes *CYC1* and *UBE2D2* were selected using a geNorm kit (Primer Design) and qBase+ software (Biogazelle; Zwijnaarde, Belgium). Using the average Cq of *CYC1* and *UBE2D2* for normalization, mRNA relative expression level was calculated by the $2^{-\Delta\Delta Cq}$ method.

ELISA

HDFs were plated on collagen I–coated (30 μgml^{-1}, Invitrogen) 6-well plates and incubated for 24 hours in fibroblast complete medium to 80% confluency, and then washed and serum-starved for 24 hours before incubation with SFM alone or SFM containing 10 μM Salbutamol for 6 or 24 hours. Supernatant growth factor levels were determined using human Duoset ELISA kits (R&D Systems).

Immunocytochemistry

SMA Immunocytochemistry: 8,500 HDFcm^{-2} were plated on sterile coverslips for 24 hours in fibroblast complete medium, then serum-starved, overnight. Pretreatment was applied for 6 hours with either SFM alone or SFM containing Formoterol/Salbutamol (10 μM), TGFβ1 (1 ng/ml), FGF2 (10 ng/ml), or PD173074 (50 nM), before adding TGFβ1 (1 ng/ml) or Salbutamol (10 μM) for a further 42 hours, as per combinations stated in the figures. sp-cAMP or rp-cAMP (50 μM) were applied for 30 minutes before treatment with SFM alone or SFM containing 10 μM Salbutamol for 2 hours. Cells were fixed in ice-cold methanol for 10 minutes and blocked for 1 hour with 2% donkey serum/5% BSA.

Vinculin Immunocytochemistry (FAs): 2,150 HDF/cm^2 were plated and serum-starved as above. Pretreatment was applied for 30 minutes in SFM alone or SFM containing PD173074 (50 nM), sp-cAMP (50 μM), or rp-cAMP, before treatment with Salbutamol (10 μM) or FGF2 (10 ng/ml) for 15 minutes. Cells were fixed in 4% paraformaldehyde (10 minutes), permeabilized in 0.1% Triton X-100 (5 minutes), and blocked (1 hour) with 5% donkey serum.

Mouse anti-SMA (1:500, A2547, Sigma) or anti-vinculin antibody (1:100, V9131, Sigma) were incubated for 2 hours at room temperature, followed by incubation with Alexa Fluor 488 donkey anti-mouse IgG secondary antibody (1:500, A-21202, Invitrogen) for 1 hour. Coverslips were mounted using ProLong Gold containing DAPI (Invitrogen). Image acquisition was performed on a Nikon Eclipse TE2000-E microscope using the Volocity software (Improvision, Perkin Elmer).

Analyses were performed on 20 separate random fields from duplicate samples, per condition. The mean ratio of SMA-positive HDFs/total HDFs was determined using Volocity, counting total DAPI-stained nuclei and SMA-positive HDF numbers, within defined fluorescence thresholds in blue and green channels, respectively. On 20 HDF per experiment ($n=4$), FAs were counted and measured manually on calibrated pictures using Volocity, then classified according to their length: immature (<4 μm), mature (4–8 μm) and supermature FAs (>8 μm) (Dugina *et al.*, 2001). Only peripheral FAs were measured.

Scar protocol

Ten Red Durocs were fasted for 12 hours before surgery and provided premedication/anesthesia and analgesia as advised by the vet. Premedication comprised detomidine (0.1 mgkg^{-1}; Orion Pharma, Newbury, UK), ketamine (5 mgkg^{-1}; Vetoquinol, Buckingham, UK), and buprenorphine (0.05 mgkg^{-1}; Animalcare Ltd, York, UK); anesthesia included alfaxan (0.7–2.4 mgkg^{-1}; Jurox, Malvern, UK) and inhaled isoflourane (Abbot Laboratories, Maidenhead, UK). Lidocaine hydrocholride (1% w/v; Hameln Pharmaceuticals, Gloucester, UK) was administered directly into wounds after surgery. Buprenorphine (0.05 mgkg^{-1}) was provided intramuscularly every 8 hours, and meloxicam (0.4 mgkg^{-1}; Boehringer Ingelheim, Bracknell, UK) was provided intramuscularly, daily, for the first 48 hours post surgery and then was administered orally, daily (0.4 mgkg^{-1}).

Animals were placed in ventral recumbency, and their backs were shaved and washed with skin prep. Twenty 2 × 2 cm^2 full-thickness wounds were created in 5 rows and 4 columns down the back, with a minimum of 2.5 cm between each wound (Figure 4a) (Gallant-Behm *et al.*, 2008). Using a scalpel and metal guide, the skin, including subcutaneous fat, was removed exposing the underlying fascia. Wound corners and the edge centers were marked with ink tattoos and animals were randomized into two groups. A volume of 500 μl of Granugel (Convatec, Uxbridge, UK) diluted 2:1 in sterile water, alone (controls) or containing 5 mM Salbutamol sulfate (1.2 mgml^{-1} Salbutamol), was freshly prepared and added to each wound after surgery and daily thereafter.

Wounds were covered with a new dressing daily (Steroplast, Manchester, UK) and custom jackets (Agenda Group, Hull, UK) for study duration.

On days 7,14,21,28,42 post wounding, animals were provided with analgesia/anesthesia, skin was shaved, each wound was digitally photographed, and four 6-mm punch biopsies (Miltex, Weymouth, UK) were taken from 2 wounds/animal, as shown in (Figure 4a). On day 56 post wounding, animals were provided with analgesia/anesthesia, skin was shaved, and each wound was digitally photographed and assessed for scar appearance. Animals were then euthanized using a schedule 1 method, and the remaining ten scars/animal were harvested for histology.

Wound healing and scar formation assessment

Wound healing and scar area were analyzed from calibrated wound photographs in a double-blind manner, using Adobe Photoshop. Wound area was measured from day 7 to day 28, using the wound

edges marked by tattoos. Re-epithelialized area was calculated at days 14/28 by measuring the non-re-epithelialized area of the wound, dividing it by the wound area at day 0, and multiplying it by 100, to obtain the percentage non-re-epithelialized area, which was then subtracted from 100 to give % re-epithelialization.

Visible scar area was measured from day 28 to day 56. Hyperpigmented, red, raised, or damaged skin at the wound site was included in the scar area. Scar assessment was performed at day 56 before animal euthanasia using a composite of the Manchester (Beausang *et al.*, 1998) and Vancouver (Sullivan *et al.*, 1990) scar scales with modifications for porcine wounds (Supplementary Table S1 online). The results are presented as mean values/scores +/− SEM ($n=10$ for biopsies; $n=50$ for excised scars).

Immunohistochemistry

Excised biopsies were snap-frozen in liquid nitrogen, whereas excised scars were halved along the cranial–caudal axis and embedded in Tissue Tek OCT compound (Sakura Finetek, Thatcham, UK) before freezing in isopentane. 10-μm-thick frozen sections were air-dried for 30 minutes and fixed in acetone, before staining with H&E or Masson's trichrome. Macrophage infiltration was detected by α-NAE staining (kit 91-A, Sigma-Aldrich). Immunohistochemistry was performed on acetone-fixed sections using the Histostain-Plus IHC Detection Kit (Invitrogen) with anti-vWF ab6994 (Abcam, Cambridge, UK), anti-SMA (A2547, Sigma), anti-FN EDA ab6328, anti-COL1 ab90395, anti-FGF2 ab181, anti-collagen III ab23445, anti-CCN2 ab6992, and anti-CD163 MCA2311GA (Serotec, Hemel Hempstead, UK), and incubated overnight at 4 °C. Sections were counterstained with Mayer's haematoxylin before dehydration and mounting.

Brightfield pictures of scar sections were acquired on a Zeiss Axiovert 200 microscope with the Axiovision 4.8 software using multiacquisition stitching. Calibrated images were analyzed with Adobe Photoshop (Maidenhead, UK). Neo-collagen fiber deposition was determined by measuring collagen fiber negative areas (red), within the dermis (defined from H&E sections), in the Masson's trichrome staining. Neo-angiogenesis was determined by the number of discrete vWF-stained structures counted within a 0.25 mm^2 (biopsies) or 1 mm^2 (excised scars) area within the most densely stained area (biopsies) or wound bed directly below the epidermis (excised scars). Inflammation was assessed by the % macrophage-infiltrated area of the biopsy (NAE/anti-CD163 staining) or wound bed (excised scars). The wound bed on excised scar sections was defined from H&E-stained sections and demarcated on Figure 5d–h and Supplementary Figure S4a and b online with a black line.

Statistical analysis

Statistical significance was analyzed using the GraphPad Prism6 software (La Jolla, CA). Data distribution was first assessed using the D'Agostino & Pearson normality test. Continuous variables were analyzed with the two-tailed unpaired Student's *t*-test (Gaussian distributions), with a Welch's correction for unequal variances when necessary, or with the nonparametric Mann–Whitney test (non-Gaussian distributions). One or two categorical variables were analyzed by one-way or two-way ANOVA (Gaussian distributions), with the Bonferroni's post-test, or by the Kruskal–Wallis test (non-Gaussian distributions) with a Dunn's post-test. Values are presented as mean +/− SEM, with statistical significance ascribed as $*P<0.05$/$**P<0.01$/$***P<0.001$.

CONFLICT OF INTEREST

The authors state no conflict of interests.

ACKNOWLEDGMENTS

This work was supported by a Wellcome Trust (http://www.wellcome.ac.uk) grant 82586 (CEP), an MRC (http://www.mrc.ac.uk) grant G0901844 (CEP), and a BSF (http://www.britishskinfoundation.org.uk) grant 929 s (CEP). The authors thank Andy O'Leary for his help with the CAM assay, Francis Pollen for his help with HDF focal adhesion analysis, Jonathan McDearmid for his help with staging the zebrafish embryos, David Read for his help with capture of the histology images, and James Fox for proof-reading the manuscript, all from the University of Leicester.

AUTHOR CONTRIBUTIONS

CEP initiated the concept for all mechanistic studies, designed, acquired, analyzed and interpreted some of the data, and drafted and revised the article. GSLP substantially contributed to the design of some experiments, the acquisition, analysis, and interpretation of the majority of the associated data, and the drafting and proofreading of the article.

SUPPLEMENTARY MATERIAL

Supplementary material is linked to the online version of the paper at http://www.nature.com/jid

REFERENCES

Ausprunk DH, Knighton DR, Folkman J (1974) Differentiation of vascular endothelium in the chick chorioallantois: a structural and autoradiographic study. *Dev Biol* 38:237–48

Baker JG (2010) The selectivity of beta-adrenoceptor agonists at human beta1-, beta2- and beta3-adrenoceptors. *Br J Pharmacol* 160:1048–61

Bayat A, McGrouther DA, Ferguson MW (2003) Skin scarring. *BMJ* 326: 88–92

Beausang E, Floyd H, Dunn KW *et al.* (1998) A new quantitative scale for clinical scar assessment. *Plast Reconstr Surg* 102:1954–61

Boskabady MH, Saadatinejad M (2003) Airway responsiveness to beta-adrenergic agonist (salbutamol) in asthma. *J Asthma* 40:917–25

Braun LR, Lamel SA, Richmond NA *et al.* (2013) Topical timolol for recalcitrant wounds. *JAMA Dermatol* 149:1400–2

Chen W, Fu XB, Ge SL *et al.* (2006) Analysis of differentially expressed genes in fetal skin of scarless and scar-forming periods of gestational rats. *Chin J Traumatol* 9:94–9

Denda M, Fuziwara S, Inoue K (2003) Beta2-adrenergic receptor antagonist accelerates skin barrier recovery and reduces epidermal hyperplasia induced by barrier disruption. *J Invest Dermatol* 121:142–8

DiPietro LA (2013) Angiogenesis and scar formation in healing wounds. *Curr Opin Rheumatol* 25:87–91

Dostmann WR, Taylor SS, Genieser HG *et al.* (1990) Probing the cyclic nucleotide binding sites of cAMP-dependent protein kinases I and II with analogs of adenosine 3′,5′-cyclic phosphorothioates. *J Biol Chem* 265: 10484–91

Dugina V, Fontao L, Chaponnier C *et al.* (2001) Focal adhesion features during myofibroblastic differentiation are controlled by intracellular and extracellular factors. *J Cell Sci* 114:3285–96

Fairbairn L, Kapetanovic R, Beraldi D *et al.* (2013) Comparative Analysis of Monocyte Subsets in the Pig. *J Immunol* 190:6389–96

Fantin A, Vieira JM, Gestri G *et al.* (2010) Tissue macrophages act as cellular chaperones for vascular anastomosis downstream of VEGF-mediated endothelial tip cell induction. *Blood* 116:829–40

Gallant CL, Olson ME, Hart DA (2004) Molecular, histologic, and gross phenotype of skin wound healing in red Duroc pigs reveals an abnormal healing phenotype of hypercontracted, hyperpigmented scarring. *Wound Repair Regen* 12:305–19

Gallant-Behm CL, Hart DA (2006) Genetic analysis of skin wound healing and scarring in a porcine model. *Wound Repair Regen* 14: 46–54

Gallant-Behm CL, Hildebrand KA, Hart DA (2008) The mast cell stabilizer ketotifen prevents development of excessive skin wound contraction and fibrosis in red Duroc pigs. *Wound Repair Regen* 16:226–33

Hayward PG, Robson MC (1991) Animal models of wound contraction. *Prog Clin Biol Res* 365:301–12

Hinz B (2007) Formation and function of the myofibroblast during tissue repair. *J Invest Dermatol* 127:526–37

Hinz B, Celetta G, Tomasek JJ *et al.* (2001) Alpha-smooth muscle actin expression upregulates fibroblast contractile activity. *Mol Biol Cell* 12:2730–41

Insel PA, Murray F, Yokoyama U *et al.* (2012) Cyclic AMP and Epac in the regulation of tissue fibrosis. *Br J Pharmacol* 166:447–56

Ishiguro S, Akasaka Y, Kiguchi H *et al.* (2009) Basic fibroblast growth factor induces down-regulation of alpha-smooth muscle actin and reduction of myofibroblast areas in open skin wounds. *Wound Repair Regen* 17:617–25

Kimmel CB, Ballard WW, Kimmel SR *et al.* (1995) Stages of embryonic development of the zebrafish. *Dev Dyn* 203:253–310

Kratz G (1998) Modeling of wound healing processes in human skin using tissue culture. *Microsc Res Tech* 42:345–50

Lev-Tov H, Dahle S, Moss J *et al.* (2013) Successful treatment of a chronic venous leg ulcer using a topical beta-blocker. *J Am Acad Dermatol* 69:e204–5

Levesque M, Feng Y, Jones RA *et al.* (2013) Inflammation drives wound hyperpigmentation in zebrafish by recruiting pigment cells to sites of tissue damage. *Dis Model Mech* 6:508–15

Lucas T, Waisman A, Ranjan R *et al.* (2010) Differential roles of macrophages in diverse phases of skin repair. *J Immunol* 184:3964–77

Manahan MN, Peters P, Scuderi S *et al.* (2014) Topical timolol for a chronic ulcer–a case with its own control. *Med J Aust* 200:49–50

Margolis DJ, Hoffstad O, Isseroff RR (2007) Association between the use of beta-adrenergic receptor agents and the development of venous leg ulcers. *Arch Dermatol* 143:1275–80

Miyake M, Ishii M, Koyama N *et al.* (2010) 1-tert-butyl-3-[6-(3,5-dimethoxy-phenyl)-2-(4-diethylamino-butylamino)-pyrido[2,3-d]pyrimidin-7-yl]-urea (PD173074), a selective tyrosine kinase inhibitor of fibroblast growth factor receptor-3 (FGFR3), inhibits cell proliferation of bladder cancer carrying the FGFR3 gene mutation along with up-regulation of p27/Kip1 and G1/G0 arrest. *J Pharmacol Exp Ther* 332:795–802

Montagna W, Yun JS (1964) The skin of the domestic Pig. *J Invest Dermatol* 42:11–21

Nagatsu T, Stjarne L (1998) Catecholamine synthesis and release. Overview. *Adv Pharmacol* 42:1–14

Ogawa R, Akaishi S, Huang C *et al.* (2011) Clinical applications of basic research that shows reducing skin tension could prevent and treat abnormal scarring: the importance of fascial/subcutaneous tensile reduction sutures and flap surgery for keloid and hypertrophic scar reconstruction. *J Nippon Med Sch* 78:68–76

Ono I, Akasaka Y, Kikuchi R *et al.* (2007) Basic fibroblast growth factor reduces scar formation in acute incisional wounds. *Wound Repair Regen* 15:617–23

Pullar CE, Isseroff RR (2005) Beta 2-adrenergic receptor activation delays dermal fibroblast-mediated contraction of collagen gels via a cAMP-dependent mechanism. *Wound Repair Regen* 13:405–11

Pullar CE, Grahn JC, Liu W *et al.* (2006a) Beta2-adrenergic receptor activation delays wound healing. *FASEB J* 20:76–86

Pullar CE, Rizzo A, Isseroff RR (2006b) beta-Adrenergic receptor antagonists accelerate skin wound healing: evidence for a catecholamine synthesis network in the epidermis. *J Biol Chem* 281:21225–35

Pullar CE, Manabat-Hidalgo CG, Bolaji RS *et al.* (2008) beta-Adrenergic receptor modulation of wound repair. *Pharmacol Res* 58:158–64

Pullar CE, Le Provost GS, O'Leary AP *et al.* (2012) beta2AR Antagonists and beta2AR Gene Deletion Both Promote Skin Wound Repair Processes. *J Invest Dermatol* 132:2076–84

Redd MJ, Cooper L, Wood W *et al.* (2004) Wound healing and inflammation: embryos reveal the way to perfect repair. *Philos Trans R Soc Lond B Biol Sci* 359:777–84

Renshaw SA, Loynes CA, Trushell DM *et al.* (2006) A transgenic zebrafish model of neutrophilic inflammation. *Blood* 108:3976–8

Scott MG, Swan C, Jobson TM *et al.* (1999) Effects of a range of beta2 adrenoceptor agonists on changes in intracellular cyclic AMP and on cyclic AMP driven gene expression in cultured human airway smooth muscle cells. *Br J Pharmacol* 128:721–9

Shaw TJ, Martin P (2009) Wound repair at a glance. *J Cell Sci* 122:3209–13

Sindrilaru A, Scharffetter-Kochanek K (2013) Disclosure of the culprits: macrophages-versatile regulators of wound healing. *Adv Wound Care (New Rochelle)* 2:357–68

Sivamani RK, Pullar CE, Manabat-Hidalgo CG *et al.* (2009) Stress-mediated increases in systemic and local epinephrine impair skin wound healing: potential new indication for beta blockers. *PLoS Med* 6:e12

Stramer BM, Mori R, Martin P (2007) The inflammation-fibrosis link? A Jekyll and Hyde role for blood cells during wound repair. *J Invest Dermatol* 127:1009–17

Sullivan T, Smith J, Kermode J *et al.* (1990) Rating the burn scar. *J Burn Care Rehabil* 11:256–60

Sullivan TP, Eaglstein WH, Davis SC *et al.* (2001) The Pig as a model for human wound healing. *Wound Repair Regen* 9:66–76

Szpaderska AM, Walsh CG, Steinberg MJ *et al.* (2005) Distinct patterns of angiogenesis in oral and skin wounds. *J Dent Res* 84:309–14

Takenaka H, Yasuno H, Kishimoto S (2002) Immunolocalization of fibroblast growth factor receptors in normal and wounded human skin. *Arch Dermatol Res* 294:331–8

Tang JC, Dosal J, Kirsner RS (2012) Topical timolol for a refractory wound. *Dermatol Surg* 38:135–8

Tiede S, Ernst N, Bayat A *et al.* (2009) Basic fibroblast growth factor: a potential new therapeutic tool for the treatment of hypertrophic and keloid scars. *Ann Anat* 191:33–44

Tomasek JJ, Gabbiani G, Hinz B *et al.* (2002) Myofibroblasts and mechano-regulation of connective tissue remodelling. *Nat Rev Mol Cell Biol* 3: 349–63

Tuan TL, Nichter LS (1998) The molecular basis of keloid and hypertrophic scar formation. *Mol Med Today* 4:19–24

Wallukat G (2002) The beta-adrenergic receptors. *Herz* 27:683–90

Wang ZP, Nishimura Y, Shimada Y *et al.* (2009) Zebrafish beta-adrenergic receptor mRNA expression and control of pigmentation. *Gene* 446: 18–27

Weisser SB, McLarren KW, Kuroda E *et al.* (2013) Generation and characterization of murine alternatively activated macrophages. *Methods Mol Biol* 946:225–39

Westerfield M (1994) *The Zebrafish Book: A Guide To The Laboratory Use Of The Zebrafish (Brachydanio rerio)*. 2.1 edn. Eugene: University of oregon Press

Wilgus TA, Ferreira AM, Oberyszyn TM *et al.* (2008) Regulation of scar formation by vascular endothelial growth factor. *Lab Invest* 88:579–90